Difference equation approach to two-thermocouple sensor characterization in constant velocity flow environments

P. C. Hung, G. Irwin, and R. Kee[a]
Virtual Engineering Centre, Queen's University Belfast, Belfast BT9 5HN, Northern Ireland

S. McLoone
Department of Electronic Engineering, National University of Ireland, Maynooth, Maynooth, Co. Kildare, Ireland

Thermocouples are one of the most popular devices for temperature measurement due to their robustness, ease of manufacture and installation, and low cost. However, when used in certain harsh environments, for example, in combustion systems and engine exhausts, large wire diameters are required, and consequently the measurement bandwidth is reduced. This article discusses a software compensation technique to address the loss of high frequency fluctuations based on measurements from two thermocouples. In particular, a difference equation (DE) approach is proposed and compared with existing methods both in simulation and on experimental test rig data with constant flow velocity. It is found that the DE algorithm, combined with the use of generalized total least squares for parameter identification, provides better performance in terms of time constant estimation without any *a priori* assumption on the time constant ratios of the thermocouples. © 2005 American Institute of Physics. [DOI: 10.1063/1.1847412]

I. INTRODUCTION

Commercial and industrial applications frequently demand accurate measurements of instantaneous temperature at certain fixed locations in engineering systems. The exact reasons for such a requirement are diverse, but generally speaking, the ability to measure such temperatures *in situ* allows a closer look into the system behavior. This can potentially provide valuable insights for engineers, including more refined performance analysis, advanced fault diagnosis and possibly improved design.

The thermocouple is a widely used device for measuring temperature due to its high permissible working limit and good linear dependence with temperature. In addition, its high robustness, low cost and ease of installation means there are many situations in which thermocouples are the only suitable type of equipment for temperature measurement.

While there are other types of thermometers, including liquid in glass, resistance, semiconductor and optical pyrometer (infrared), these are less suitable for certain engineering applications and are usually less durable and more expensive. However, the design of a thermocouple-based temperature measurement system involves a compromise between robustness and speed of response; this poses major problems when measuring high frequency temperature fluctuations. The bandwidth ω_B of a thermocouple is dependent on its wire diameter according to the equation

$$\omega_B = \kappa^{-1} d^{m-2} v^m, \tag{1}$$

where κ and m are approximately constant and arise from thermodynamic considerations, d is the diameter of the thermocouple wire and v is the velocity of the gas. Large diameter thermocouples are usually required to withstand harsh environments such as engine combustion systems, thus resulting in a low bandwidth of typically less than 1 Hz. Unfortunately, temperature variations, such as those in the exhaust of a reciprocating internal combustion engine, are usually 2–3 orders of magnitude faster which leads to raw signal measurements from the thermocouple that are both severely attenuated and lagged.

As an example, among current techniques for such fluctuating temperature measurement, up to 0.1–10 kHz in turbulent flames and other combustion environments, a fine-wire resistance thermometer of $0.6–3$ μm in diameter (usually called "cold wire") is widely used because of its fast response.[1] Here the typical bandwidth is of the order of 1 kHz but the wire is mechanically very weak and is not durable enough to withstand the high temperature of combustion. A "fine-wire" thermocouple of $20–50$ μm in diameter, on the other hand, is generally superior to a cold wire in durability, but is a slow thermometer[2] of bandwidth in the range $1–10$ Hz. In this case, appropriate compensation is required to produce accurate measurement of temperature fluctuations. Before any such compensation can be done, an acceptable model of the thermocouple is needed.

From the conservation of energy, the thermocouple heat transfer equation can be written in words as

---

[a]Author to whom correspondence should be addressed; electronic mail: r.kee@qub.ac.uk

[convective heat transfer]

= [thermal inertia]

+ [conductive and radiative heat transfer].

For well-designed thermocouples with long fine wires to minimize axial heat conduction and radiative heat transfer, it may be assumed that both the conductive and radiative heat transfers are negligible when compared to the convective heat transfer.[3–6] Therefore a first-order lag model with time constant τ and unity gain can represent the frequency response of a fine-wire thermocouple.[7–10] The simplified thermocouple model can be written mathematically as

$$T_g(t) = T_m(t) + \tau \dot{T}_m(t). \tag{2}$$

Using Eq. (2), the original gas temperature T_g can be reconstructed if τ, T_m and $\dot{T}_m$ are available. In practice, this approach is infeasible as the measured temperature may be noisy, and the derivative will be difficult to compute accurately. In addition, since the bandwidth ω_B is dependent upon gas velocity as given in Eq. (1), the time constant will vary as follows:

$$\tau = \frac{2\pi}{\omega_B} = 2\pi \kappa d^{2-m} v^{-m}. \tag{3}$$

Alternative more robust schemes for reconstruction of true gas temperature generally involve the use of two or more thermocouples with different time constants. The techniques usually involve two separate stages: estimation of time constants, followed by temperature reconstruction.

Pfriem[11] in 1936 first proposed the use of double thermocouples for temperature measurements, and since then many techniques have been developed. Time domain reconstruction (TDR)[2–4] is based on the continuous-time differential equation model, which requires numerical signal derivatives for the time constant estimations. TDR algorithms may only require an *a priori* estimate of the time constant ratio α between the two thermocouples. Frequency domain reconstruction,[5,12] on the other hand, uses the frequency component for data processing, avoiding the need to calculate unreliable derivatives from noisy temperature data. However, undesirable oscillations[4] may be introduced in the final reconstructions due to the nature of Fourier transforms and singularities due to noise. Attempts have also been made to estimate time constants from the power spectra,[13] however even moderate amounts of noise can severely corrupt the spectra.

In this article, the temperature measurements are limited to those recorded in constant velocity flow environments. The time constant is then assumed constant or approximately constant during the course of data recording. A software compensation technique based on the measurements from two thermocouples is discussed. In particular, a difference equation based algorithm is proposed which uses generalized total least squares (GTLS) for parameter identification. It is shown that this approach provides better performance in terms of time constant estimation without any *a priori* assumption on the thermocouple time constants.

II. THERMOCOUPLE CHARACTERIZATION

Unfortunately, it is extremely difficult to estimate by calculation the value of the time constant, even under the simplifying assumption that κ and m are constant. To determine these requires information on the geometric configuration of the sensor and the velocity v of the surrounding gas. Furthermore, if the time constant is to be estimated *in situ*, the velocity v may not be easily determined.

Experimentally, thermocouple time constants may be measured using a cooling curve[4,14] approach. This involves passing a current through a thermocouple wire placed in an air stream of a known speed. The applied current heats up the thermocouple wires and when switched off, the air stream cools the thermocouple. This is repeated at different stream velocities to obtain a relationship between air velocity and time constant. While this method is acceptable for experimental verification purposes, it is impractical for high bandwidth thermocouples, as their cooling curves fall off too quickly.

III. PROPOSED METHOD

Hung *et al.* applied discrete-time system identification techniques to sensor characterization.[15] This has the advantage that it avoids the assumption of the time constant ratio α being time invariant and known *a priori*.

The first-order difference equation model equivalent to the single thermocouple description in Eq. (2) is given by

$$T_m(k) = aT_m(k-1) + bT_g(k-1). \tag{4}$$

Assuming zero order holds (ZOHs) and a sampling interval τ_s, the parameters of the discrete and continuous thermocouple models are related by

$$a = \exp\left(-\frac{\tau_s}{\tau}\right) \tag{5}$$

and

$$b = 1 - a. \tag{6}$$

Equation (4) is an autoregressive with exogenous input (ARX) model[16] and its parameters could be estimated using least squares from an appropriate set of input-output samples as will be discussed further in the next section. Unfortunately, in this application $T_g(k-1)$ is unknown, hence a and b cannot be determined directly. However, a two-thermocouple based identification method can be developed using the ARX model as follows:

$$T_{m1}(k) = a_1 T_{m1}(k-1) + (1-a_1)T_g(k-1),$$

$$T_{m2}(k) = a_2 T_{m2}(k-1) + (1-a_2)T_g(k-1). \tag{7}$$

Two difference equation methods have been developed: a three-parameter and a two-parameter method, denoted the gamma and the beta methods, respectively.

A. Gamma least-squares approach

The temperature $T_g(k-1)$ can be eliminated from Eq. (7) to yield the following relationship between the thermocouple outputs:
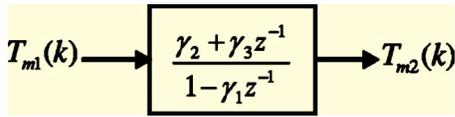
FIG. 1. Equivalent ARX model for two-thermocouple parameter identification.

$$T_{m2}(k) = a_2 T_{m2}(k-1) + \frac{(1-a_2)}{(1-a_1)} T_{m1}(k)$$

$$- \frac{a_1(1-a_2)}{(1-a_1)} T_{m1}(k-1). \qquad (8)$$

Note that Eq. (8) is nonlinear in the unknown parameters. By minimizing the mean-square prediction error over N samples, defined as

$$J(a_1, a_2) = \frac{1}{N} \sum_{k=1}^{N} (T_{m2}(k) - \hat{T}_{m2}(k))^2, \qquad (9)$$

where $\hat{T}_{m2}(k)$ is the prediction generated by Eq. (8), parameters a_1 and a_2 can now be identified. However, since this would require the use of nonlinear optimization, a better approach is to convert Eq. (8) into a three-parameter representation by defining

$$\gamma_1 = a_2, \quad \gamma_2 = \frac{1-a_2}{1-a_1} \text{ and } \gamma_3 = -a_1 \frac{1-a_2}{1-a_1}. \qquad (10)$$

Equation (8) can then be written as

$$T_{m2}(k) = \gamma_1 T_{m2}(k-1) + \gamma_2 T_{m1}(k) + \gamma_3 T_{m1}(k-1). \qquad (11)$$

By choosing $T_{m2}(k)$ as the output variable and $T_{m1}(k)$ as the input variable, the ARX structure illustrated in Fig. 1 is obtained. Conventional linear identification such as least squares can now be used to determine the estimates $\hat{\gamma}_1$, $\hat{\gamma}_2$, and $\hat{\gamma}_3$, and hence the thermocouple parameters via Eq. (10).

This difference equation approach relies on identification of an ARX sensor model in which both the input and output signals are subject to noise (assumed to be zero-mean Gaussian and white). Conventional least squares will produce bi-

ased parameter estimates since the input data are noisy. Other models, which take account of colored noise on the output, such as auto-regressive with moving average exogenous input (ARMAX) and output error (OE) were shown[17] to indeed give significant reductions in bias. However, these all also assume a noise-free input in Fig. 1.

B. Gamma total least-squares approach

To further improve difference equation model based sensor characterizations, both input and output noise must be dealt with simultaneously. Total least squares (TLS), a least squares formulation which takes account of noise present on both input and output signals, was investigated by Hung *et al.*[17] in this context. The TLS solution, which is easily computed using singular value decomposition (SVD),[18] produces unbiased estimates, provided the noise variances on both input and output signals in Fig. 1 are the same.[18] This is usually the case in a well-designed thermocouple measurement system, assuming only a background noise source.

Unfortunately, while TLS estimates are unbiased, they tend to have a larger variance than LS estimates, with the result that in some situations the performance can in fact be worse than that of LS. Also, TLS has been found to be less robust than LS because it is more sensitive to assumptions about the noise.[19] Further, Eq. (10) provides an overdetermined three-parameter relationship to the parameters a_1 and a_2 so that multiple sets of parameter solutions are possible. To determine $\hat{\tau}_1$ and $\hat{\tau}_2$, it is therefore necessary either to assume that only one set of the parameter estimates is correct or perform a nonlinear optimization.

C. Beta least-squares approach

Defining

$$\beta = b_2/b_1, \qquad (12)$$

Eq. (8) is now reorganized to one containing only the two parameters b_1 and β in the output $T_{m2}(i)$ for $i = k, k-1, \ldots, 2$ as shown in Eq. (13):

$$T_{m2}(k) = (1-b_1\beta)T_{m2}(k-1) + \beta T_{m1}(k) - \beta(1-b_1)T_{m1}(k-1),$$

$$\vdots$$

$$T_{m2}(k-i) = (1-b_1\beta)T_{m2}(k-i-1) + \beta T_{m1}(k-i) - \beta(1-b_1)T_{m1}(k-i-1), \qquad (13)$$

$$\vdots$$

$$T_{m2}(2) = (1-b_1\beta)T_{m2}(1) + \beta T_{m1}(2) - \beta(1-b_1)T_{m1}(1).$$

Equation (13) can be rewritten in vector-matrix form as

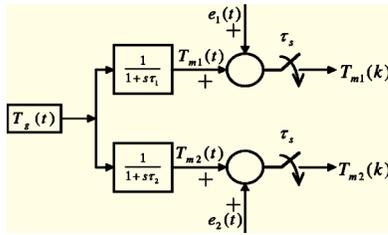$$\mathbf{Y} = \mathbf{X}\boldsymbol{\theta}, \qquad (14)$$

where

FIG. 2. Block diagram representation of the simulated two-thermocouple measurement system.

$$\mathbf{Y} = [\mathbf{T}_{m2}(k) - \mathbf{T}_{m2}(k-1)];$$

$$\mathbf{X} = [\mathbf{T}_{m1}(k) - \mathbf{T}_{m1}(k-1)\ \mathbf{T}_{m1}(k-1) - \mathbf{T}_{m2}(k-1)];$$

$$\boldsymbol{\theta} = [\theta_1\ \theta_2]^T \triangleq [\beta\ b_1\beta]^T; \tag{15}$$

$$\mathbf{T}_{mp}(k-i) = [T_{mp}(k-i)\ T_{mp}(k-i-1)\ T_{mp}(k-i-2)$$
$$\cdots\ T_{mp}(k-i-N+1)]^T.$$

The least-squares estimate of $\boldsymbol{\theta}$ then follows directly as

$$\hat{\boldsymbol{\theta}} = [\hat{\theta}_1\ \hat{\theta}_2]^T = (\mathbf{X}^T\mathbf{X})^{-1}\mathbf{X}^T\mathbf{Y}. \tag{16}$$

The parameters in Eq. (13) are then given by

$$\hat{\beta} = \hat{\theta}_1$$

and $\hat{b}_1 = \hat{\theta}_2/\hat{\theta}_1$. $\tag{17}$

There are various advantages in this so-called beta least-squares method. First, it involves estimating two parameters. This means that there are no over-determined ARX parameters. The thermocouple time constants $\hat{\tau}_1$ and $\hat{\tau}_2$ can now be obtained directly, using Eq. (5) and Eq. (6). Second, the algorithm is believed to be more resilient to background measurement noise and numerical errors than those used in Secs. III A and III B. One reason for this is that the use of β, which is almost constant (proof in the Appendix), enables more stable $\boldsymbol{\theta}$ optimization. In contrast, a_1 and a_2 vary in a larger range.

D. Beta generalized total least-squares approach

The beta approach described in the last section can be extended so that total least squares can be used for parameter estimation. However, simulation studies to be presented in Sec. IV A reveal that the beta total least-squares estimates were still biased, even when the measurement noise on each thermocouple was independent and of equal variance. A detailed analysis[20] shows that due to the way $\mathbf{X}$ and $\mathbf{Y}$ are constructed in β-TLS, the resulting noise covariance matrix $\mathbf{C}$ no longer meets the requirements for unbiased parameter estimations, i.e., it can no longer be expressed as $\mathbf{C} = v\mathbf{I}$, where v is a scalar and $\mathbf{I}$ is the identity matrix.

Generalized total least squares (GTLS), on the other hand, which employ generalized singular value decomposition (GSVD), can produce unbiased parameter estimates under these conditions provided $\mathbf{C}$ is known. The idea here is to transform the augmented SVD matrix $\mathbf{S}$ to the GSVD matrix $\mathbf{S}_G$ using a weighting matrix $\mathbf{W}$ so that the resulting transformed noise covariance matrix $\mathbf{C}_W = [\mathbf{W}^{-1}]^T\mathbf{C}[\mathbf{W}^{-1}]$ meets the unbiasedness requirement. This is achieved by defining $\mathbf{W}$ as

$$\mathbf{C}_0 = \mathbf{W}^T\mathbf{W}, \tag{18}$$

where $\mathbf{C}_0$ is proportional to the noise covariance matrix $\mathbf{C}$ (i.e., $\mathbf{C} = \mu\mathbf{C}_0$, μ an arbitrary scalar). The required weighting matrix $\mathbf{W}$ is given by the Cholesky decomposition of $\mathbf{C}_0$. Although in most cases the noise variances from the two-thermocouple signals are unknown, it is still possible to express $\mathbf{C}_0$ as a matrix function of ϕ, the ratio of those noise variances,[20] as follows:

$$\mathbf{C}_0(\phi) = \begin{bmatrix} 2\phi & -\phi & 0 \\ -\phi & \phi+1 & 1 \\ 0 & 1 & 2 \end{bmatrix}, \quad \phi > 0. \tag{19}$$

It is safe to assume ϕ to be unity in practice since the noise variances of both thermocouple outputs are usually equal. Thus the GSVD is given by

$$\mathbf{S}_G = [\mathbf{X}; \mathbf{Y}] = \mathbf{U}_G\boldsymbol{\Sigma}_S\mathbf{G}^{-1},$$

$$\mathbf{W} = \mathbf{V}_G\boldsymbol{\Sigma}_W\mathbf{G}^{-1}, \tag{20}$$

$$\boldsymbol{\Sigma}_G^2 = \boldsymbol{\Sigma}_S^T\boldsymbol{\Sigma}_S[\boldsymbol{\Sigma}_W^T\boldsymbol{\Sigma}_W]^{-1},$$

where $\mathbf{U}_G$ is $(N-1\times 3)$, $\mathbf{V}_G$ is (3×3), $\mathbf{G}$ is (3×3) and are all orthogonal matrices while $\boldsymbol{\Sigma}_G$, $\boldsymbol{\Sigma}_S$, and $\boldsymbol{\Sigma}_W$ are all (3×3) diagonal matrices. In particular, $\boldsymbol{\Sigma}_G$ contains the gener-
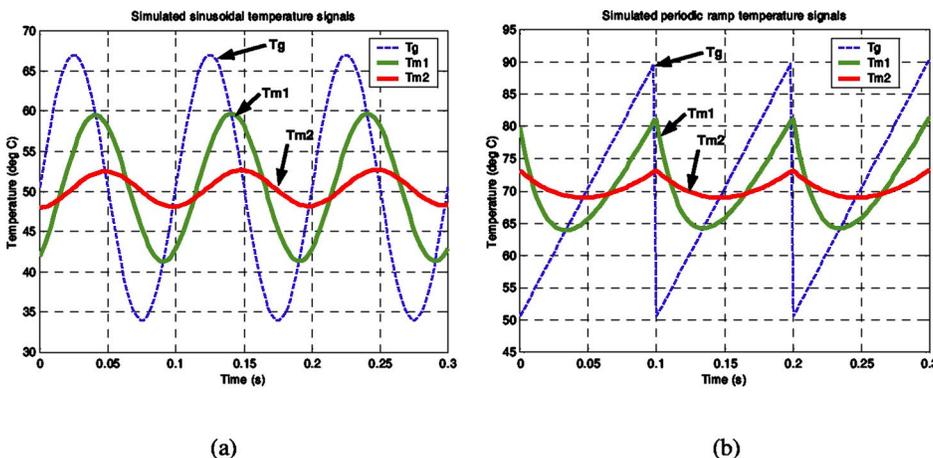

FIG. 3. (Color online) Simulated (a) sinusoidal and (b) periodic ramp gas temperatures and the corresponding thermocouple outputs (time constants are 0.0238 and 0.1168 s, respectively).
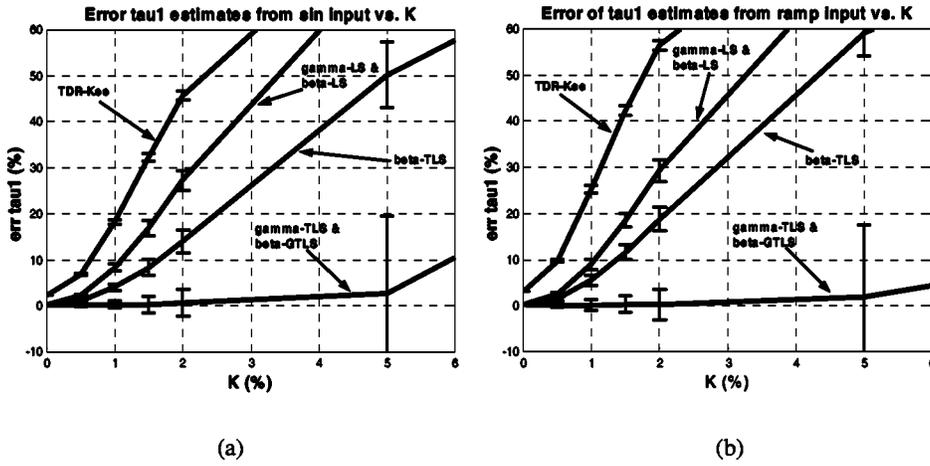
FIG. 4. Mean and standard deviation of percentage errors of $e_{\tau 1}$ against noise relative to signal K from (a) sinusoidal and (b) ramp signals, respectively.

alized singular values and the corresponding generalized singular vectors are contained in the matrix $\mathbf{G} = [\mathbf{g}_1 \ \mathbf{g}_2 \ \mathbf{g}_3]$. Therefore the GTLS solution is given as

$$[\hat{\boldsymbol{\theta}}; -1]^T = -\frac{1}{g_{3,3}} \cdot \mathbf{g}_3, \tag{21}$$

where $\mathbf{g}_3$ is the vector associated with the smallest generalized singular value and $g_{3,3}$ is the last element of $\mathbf{g}_3$. Again, the difference equation parameters $\hat{\beta}$ and $\hat{b}_1$ can be determined using Eq. (17) as in Sec. III C.

The gas temperature T_g can be estimated directly by substituting the difference equation parameters into the corresponding difference equations.

IV. SIMULATION RESULTS

Two simulation tests were conducted to evaluate the performance of the algorithms under ideal conditions. The noises added to the two thermocouple measurements were both (i) zero-mean, Gaussian sequences and (ii) with equal variances. The first assumption is not always the case practically. As discussed earlier, the second assumption is of par-
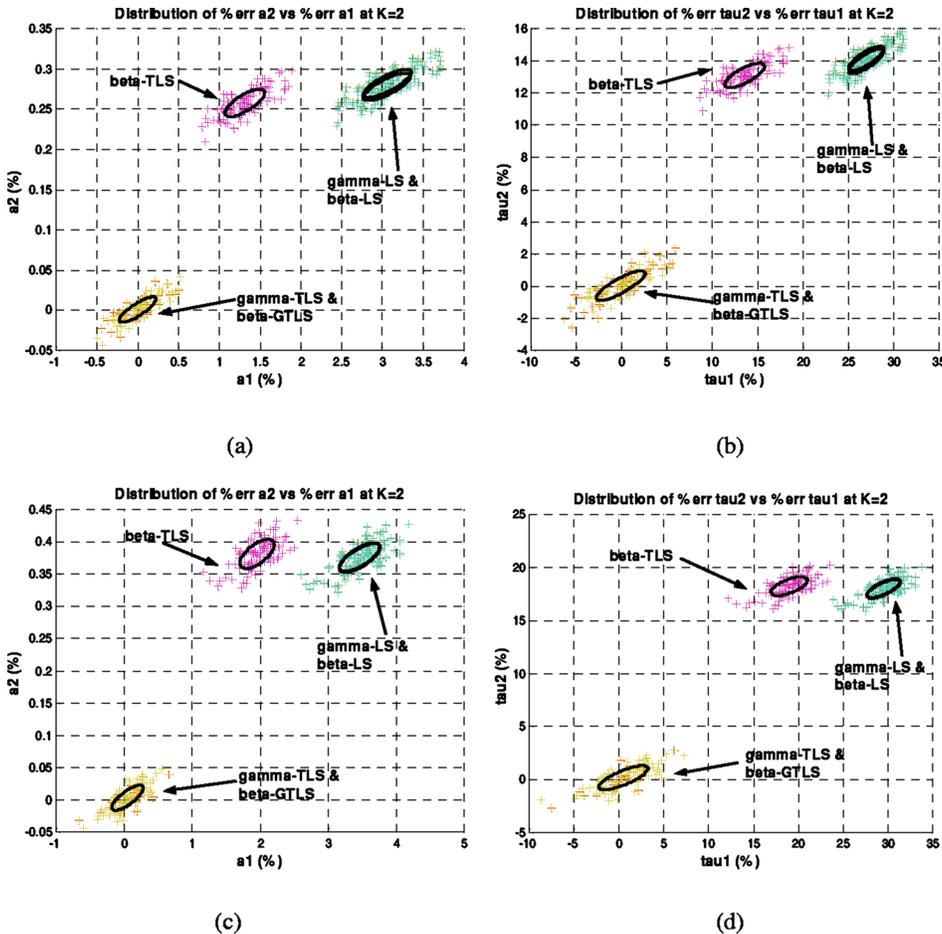

FIG. 5. (Color online) Distribution of percentage errors of $\hat{a}_2$ vs $\hat{a}_1$ [Eq. (23)] and $\hat{\tau}_2$ vs $\hat{\tau}_1$ from different algorithms at noise level $K=2$ for (a) and (b) sinusoidal and for (c) and (d) ramp signals, respectively. TDR-Kee distributions were outside the range and are thus omitted.
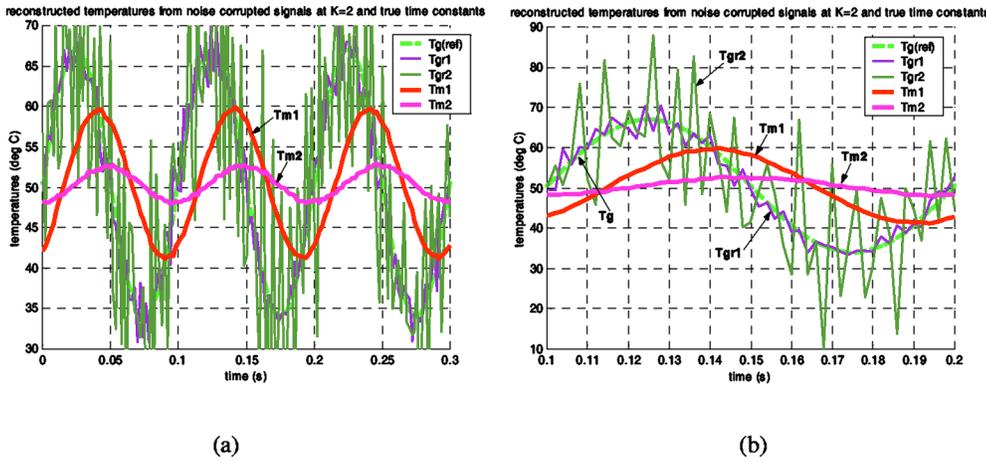
FIG. 6. (Color online) Sinusoidal temperature reconstructions from noise corrupted thermocouple outputs at $K=2$ and true time constant; (b) is a close-up version of (a) between 0.1 and 0.2 s. "Tgr1" and "Tgr2" are the reconstructions from thermocouple outputs 1 and 2, respectively.

ticular importance to the stability and accuracy of TLS parameter estimation. Simulations were based on the Matlab® Simulink model shown in Fig. 2. The thermocouples were modeled as low-pass filters with unity gain and different time constants. Noise was added after the gas temperature signal was filtered by each thermocouple. The noises added to both thermocouple outputs were not correlated.

A. Variation of average time constant estimates with noise level

The first test is the study of the resilience of the algorithms to the level of measurement noise K. Here K is defined as the percentage rms noise, as given by

$$K = \frac{100Q_{\text{rms}}}{(P - \bar{P})_{\text{rms}}} = 100\sqrt{\frac{\text{var}(Q)}{\text{var}(P)}}, \tag{22}$$

where P and Q are generic signal and noise sources, respectively.

For a given noise level, the performance of each algorithm was assessed in terms of the percentage estimation error $e_{\tau n}$, defined as

$$e_{\tau n} = \frac{100(\tau_n - \hat{\tau}_n)}{\tau_n}. \tag{23}$$

Each simulation run lasted for 10 s. A sinusoidal signal and a periodic ramp signal were each used as input gas temperatures. For clarity, Figs. 3(a) and 3(b) show only three

cycles of these two inputs and the corresponding thermocouple outputs for time constant values of 0.0238 and 0.1168 s. The outputs of the two thermocouples are significantly attenuated and phase shifted as compared to the gas inputs. The sinusoidal input and the time constant values were chosen to resemble the experimental test rig conditions (see Sec. V). Zero-mean Gaussian white noise sequences were added to both thermocouple signals in each run. The noise power was chosen to give K values in the range 0%–6%. For each K, the percentage estimation errors $e_{\tau 1}$ and $e_{\tau 2}$ from Eq. (23) in 100 runs were averaged and recorded, along with their corresponding standard deviations. Figure 4 shows the results for both temperature signals with a sampling interval of 0.002 s for all the difference equation based time constant estimation algorithms given in Sec. III. For comparison, results are included for the time derivative algorithm by Kee *et al.* (hereafter denoted TDR-Kee[4]), in which it is assumed that that the ratio of the two time constants is known *a priori*, and a sliding window with polynomial smoothing is used to get improved derivative estimates. Within each window, the time constants are estimated from an analytical expression that was derived by minimizing the time-averaged difference between two reconstructed temperatures given by the continuous-time domain model of Eq. (2). These time constants are then used to give two reconstructions from the measured data. These should be close, but not necessarily equal—the reconstructed temperature
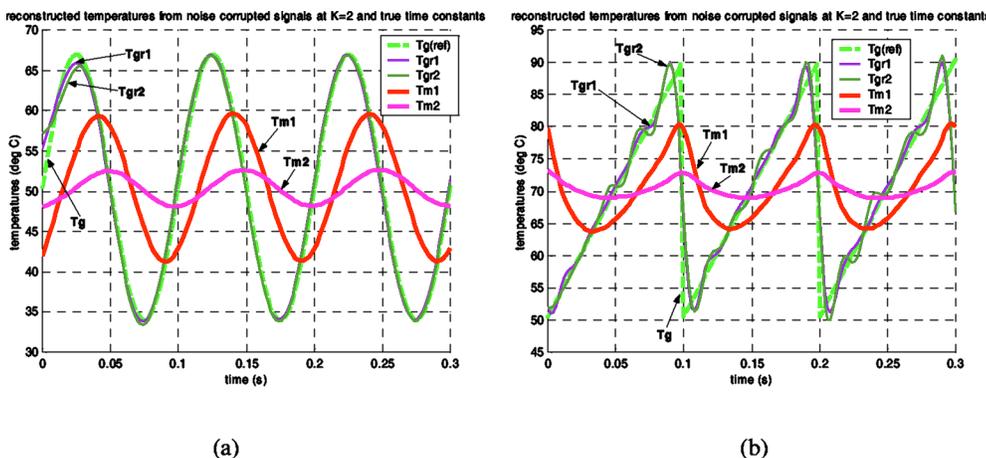

FIG. 7. (Color online) Portions of *postfiltered* (a) sinusoidal and (b) period ramp temperature reconstructions from noise-corrupted thermocouple outputs at $K=2$ and true time constants. The filter bandwidths are (a) 20 and (b) 50 Hz, respectively.
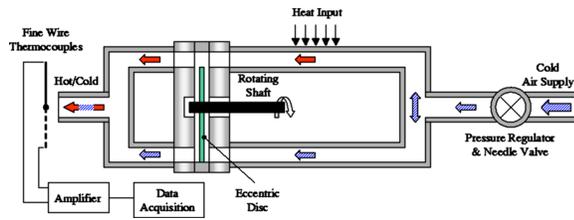
FIG. 8. (Color online) Schematic illustration of test rig.

may be taken as an average, or the reconstruction from the thermocouple with the smaller time constant.

The pattern of biases and variances can be easily seen in Fig. 5, where sample distributions of $\hat{a}_1$ and $\hat{\tau}_1$ are shown. The centers and radii of the ellipses represent the means and standard deviations of the percentage estimation errors, respectively. Note that results from TDR-Kee are all out of range. Note also that the normally distributed noise leads to ARX parameter estimates that are normally distributed, but that the time constant estimates are not normally distributed because they are obtained from the nonlinear transformation in Eq. (5).

The simulation results show that all the difference equation methods outperformed TDR-Kee. In particular, the TLS parameter estimates were less biased than their LS counterparts. The γ-LS and β-LS methods gave equal biases, while β-TLS produced slightly less biased estimates for the faster thermocouple signals only. The performances of γ-TLS and β-GTLS, which both resulted in unbiased parameter estimates at low noise levels, can be regarded as equivalent. Their means and standard deviations for the parameter estimates were almost the same at all noise levels. It is noted that, the variances of TLS estimates are bigger than those from LS.

In addition, it seems that all algorithms were more capable of estimating larger time constant values with higher accuracies. Both the biases and standard deviations of $\hat{\tau}_2$ were generally smaller than those for $\hat{\tau}_1$.

B. Temperature reconstructions

There are many ways to reconstruct the gas temperature after thermocouple sensor characterization. This includes the time derivative method where gas temperature is estimated from the first-order thermocouple model in Eq. (2). Unfortunately, it also requires estimation of thermocouple signal derivatives using, for example, polynomial fitting[4] and could be an extra source of error if not properly performed. Alternatively, the gas temperature can be directly evaluated from the first-order difference equations along with the estimated model parameters using Eq. (7). This eliminates the need for derivative estimations.

It is obvious that very good reconstructions will be achieved when the signal is completely noise free and the correct time constants are supplied. When noisy thermocouple outputs are used, the results are worse, as shown in Fig. 6. Unwanted noise is amplified after reconstruction. Although such amplification was less apparent for the faster thermocouple, it is still undesirable. The unwanted noise can be reduced by postreconstruction filtering, or simply *postfil-*
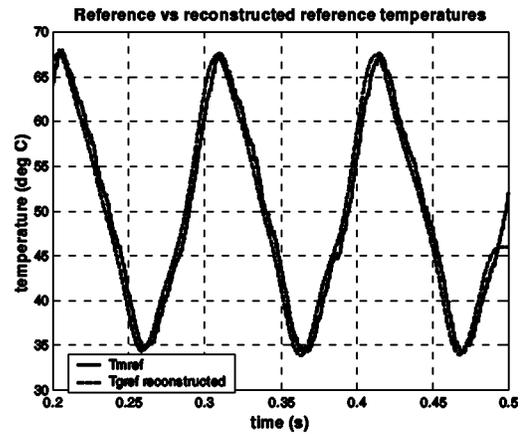

FIG. 9. Recorded $\mathbf{T}_{m\mathrm{ref}}$ and reconstructed $\hat{\mathbf{T}}_{g\mathrm{ref}}$ reference thermocouple ($\hat{\tau}_{\mathrm{ref}}=0.0026$ s) temperature signals. It is evident that due to the very small time constant, attenuation of $\mathbf{T}_{m\mathrm{ref}}$ is negligible.

tering. In this article, a fifth order Butterworth filter was used. The introduction of phase lag can be avoided using two-pass forward and backward filtering, implemented with the Matlab® command filtfilt. Figure 7 shows filtered reconstructions of both the sinusoidal and periodic ramp temperatures. For the sinusoidal signal, the filtering returned very good reconstructions, while some fluctuation remained after postfiltering in the periodic ramp reconstruction. This is because the latter contains some high frequency components which are also removed during the noise reduction process. Thus, postfiltering is a compromise between retaining high frequency temperature dynamics and noise removal.

V. RESULTS FROM TEST RIG DATA

To test the algorithms that compensate the responses from the thermocouples, experiments were carried out to collect measurements from thermocouples in an air stream with a fluctuating temperature and a constant velocity.

A. Test rig

Forney and Fralick[5] describe a constant flow temperature measurement apparatus in which a rotating wheel configuration was used to deliver a constant velocity air stream. As the wheel rotated, holes passed the two gas tubes, thereby allowing a supply of hot and cold air to alternatively enter a transition tube before reaching the thermocouples. At the thermocouples, the air flow over the thermocouples had a periodic variation in temperature.

The test rig used is illustrated in Fig. 8 and was similar to that of Forney and Fralick.[5] Cold air was supplied to the rig via a pressure regulator and a needle valve. Choked flow at the needle valve ensured that the mass flow rate was approximately constant, and only small velocity variations would arise downstream due to temperature variations. The flow was divided into two streams that were directed toward a rotating eccentric disk; one stream was heated, while the other remained at the supply temperature. As the disk rotated, varying proportions of hot and cold air were supplied to a collection tube, and directed at an array of fine thermocouples.

TABLE I. Time constant estimations and reconstruction error level of test rig data.

	TDR-Kee	γ-LS	γ-TLS	β-LS	β-TLS	β-GTLS
$\hat{\tau}_1$ (s)	0.0192	0.0228	0.0229	0.0232	0.0233	0.0233
$\hat{\tau}_2$ (s)	0.0752	0.1076	0.1078	0.1098	0.1099	0.1099
$\hat{\alpha} = \hat{\tau}_1/\hat{\tau}_2$	0.2553	0.2119	0.2124	0.2113	0.2120	0.2120
$e_{\hat{\mathbf{T}}_g}$ without postfiltering (%)	18.52	14.42	14.43	14.47	14.52	14.52
$e_{\hat{\mathbf{T}}_g}$ with postfiltering (%)[a]	19.42	15.20	15.18	15.20	15.23	15.23

[a]The postfilter bandwidth is 50 Hz.

B. Characterizations and reconstructions

In the experiments, the shaft rotated at approximately 600 rpm, to give a temperature that fluctuated at about 10 Hz. The air velocity at the thermocouples was approximately 12 m/s during data capture and the sampling interval was 0.0002 s. Wire diameters of 0.001 and 0.002 in. for T_{m1} and T_{m2}, respectively, were used. (Note that in the exhaust of an engine, such fine wires must be carefully mounted, and may only survive for several minutes. This is usually sufficient for research purposes.) To facilitate estimations using the TDR-Kee method, the time constant ratio α, defined as

$$\alpha = \frac{\tau_1}{\tau_2}, \; \tau_1 < \tau_2, \tag{24}$$

was estimated to be around 0.255 s using the ratio of instantaneous derivatives at signal crossover points.[4] Mindful of the memory requirements of SVD, only 2500 data points were used to estimate the time constants in all cases. Due to the fact that the true thermocouple time constants are unknown, there was no direct way to evaluate the performance of these algorithms on the real temperature data. However, temperature reconstructions were carried out and compared with a reference output $T_{m\text{ref}}$ from a very fine thermocouple (0.0005 in. in diameter). The time constant for the reference thermocouple $\tau_{m\text{ref}}$ was estimated to be 0.0026 s by applying the β-GTLS algorithm to T_{m1} and $T_{m\text{ref}}$. Using this time constant, the reference signal was reconstructed to give a more accurate indication of the true gas temperature. Figure 9 shows a comparison of the recorded $T_{m\text{ref}}$ and reconstructed $T_{m\text{ref}}$ reference signals, and it is evident that, due to the very small time constant, the attenuation of the signal $T_{m\text{ref}}$ from the reference thermocouple was negligible. Thus the recorded temperature $T_{m\text{ref}}$ was used as a reference, and to compare the quality of the final reconstructions $\hat{\mathbf{T}}_{g3}$, the reconstruction error level $e_{\hat{\mathbf{T}}_g}$, defined as

$$e_{\hat{\mathbf{T}}_g} = 100 \frac{[\mathbf{T}_{m\text{ref}} - \hat{\mathbf{T}}_{g3}]_{\text{rms}}}{[\mathbf{T}_{m\text{ref}}]_{\text{rms}}}, \tag{25}$$

was employed as a performance indicator.

Difference equation approach reconstructions were performed using T_{m1} and T_{m2} separately. This had the advantage over time derivative based reconstruction in that it did not require polynomial smoothing. It was found necessary to perform signal pre-conditioning before time constant estimation to achieve reasonable results. This involved pre-filtering

with a bandwidth of 100 Hz. If the signals were not filtered prior to processing, noise amplification would heavily corrupt the reconstructions.

Table I shows the time constants obtained from the five different algorithms and their corresponding reconstruction error levels. The reconstruction results, with and without postfiltering, are also displayed. The table shows that the difference equation methods performed better than the TDR one. However, the reconstruction error levels between the different difference equation methods are similar. This is because the reconstruction quality is not so sensitive to biased time constant estimation but is more affected by the noisy thermocouple measurements. The error level after postfiltering is always slightly higher than with no filtering, suggesting a compromise between reconstruction smoothness and accuracy. The reconstructions from filtering with high bandwidth contain a lot of unwanted fluctuations, while the ones from filtering with a low bandwidth are smooth sinusoids but attenuated. Note that a postfilter with a higher bandwidth allows more temperature dynamics to be retained. Thus Figs. 6 and 7 illustrate the compromises made between tolerance of noisy fluctuations and high frequency components.

Note that caution should be exercised on any conclusions drawn from these reconstruction error levels, as $\mathbf{T}_{m\text{ref}}$ is not in fact the true gas temperature which is unknown. Still, it can be observed that generally difference equation methods give improved reconstruction accuracy compared to the time derivative based approach.

To distinguish between the different difference equation methods, the time constant estimates are plotted against various pre-filter bandwidths in Fig. 10. Local maxima, found between 400 and 500 Hz, can easily be located on the graph with the various algorithms. Those are the best time constant values estimated by different algorithms from pre-filtered temperature signals. This is because on the left-hand side of the maxima, the time constants are attenuated due to a portion of the high frequency signals being removed. Erroneous estimates are found when the bandwidth cuts through the fundamental frequency (about 10 Hz), ill-conditioning all the difference equation algorithms. On the right hand side of the peaks, noise gradually erodes the estimates, a trend consistent with Fig. 4. Thus, the *best pre-filtering frequency*, which corresponds to the first major local maxima away from fundamental signal frequency on the plot, provides an alternative way to determine the quality of the time constant estimations. In Fig. 10, β-GTLS has the highest local maxima, which means it is the least affected by signal corruptions due to noise and model nonlinearity, etc. The reconstruction was
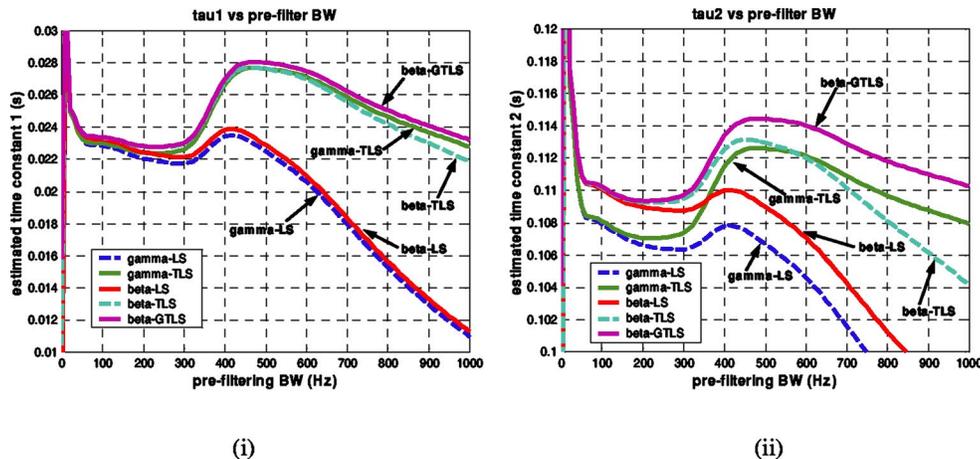
FIG. 10. (Color online) Test rig data time constant estimations vs pre-filtering bandwidth.

(i)   (ii)

most accurate using β-GTLS time constant estimates at a pre-filter bandwidth of about 470 Hz. Figure 11 shows this reconstruction from the faster thermocouple.

C. Discussion

Although the difference equation based β algorithms were shown to be better than all the other algorithms in terms of stability, it is arguable that β-GTLS only provides marginal improvements over γ-TLS when noise variances are equal, as in this application. However, in the case where the noise variance ratio ϕ is not unity, β-GTLS can easily accommodate the situation with one parameter change, but TLS cannot, and will generate biased estimates. Based on the results that both β-GTLS and γ-TLS provided equivalent consistency and unbiased estimations, plus the fact that β-GTLS is a two-parameter estimator rather than three for γ-TLS, it can be concluded that the β formulation is of better quality.

Estimated gas temperature $\hat{T}_g$ can be calculated either from the differential or difference equation with estimated time constants or model parameters. Compensated temperature $\hat{T}_g$ obtained in this way tends to amplify the noise con-

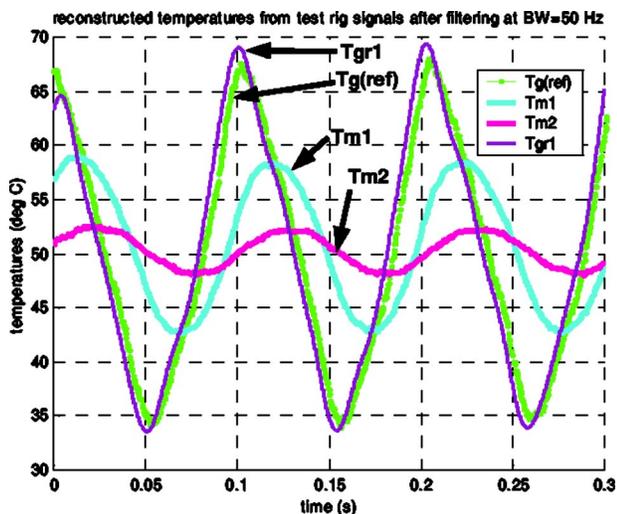FIG. 11. (Color online) Reconstruction from faster response thermocouple using β-GTLS with pre-filtering bandwidth 470 Hz and postfiltering bandwidth 50 Hz.

tained in the outputs of thermocouples. The use of *postfiltering* is found not to be the best method to eliminate the amplified noise in temperature reconstruction because such filtering also removes high frequency components of the thermocouple signals. Thus, an undesirable compromise has to be made.

APPENDIX: PROOF THAT BETA IS ALMOST INVARIANT COMPARED TO a_1 AND a_2

Recall the definition of β from Eq. (12)

$$\beta = b_2/b_1. \tag{A1}$$

Using Eq. (6), Eq. (A1) can be rewritten as

$$\beta = \frac{1-a_2}{1-a_1} = \frac{1-\exp(-\tau_s/\tau_2)}{1-\exp(-\tau_s/\tau_1)}. \tag{A2}$$

Now provided τ_s is small comparing to τ_1, i.e.,

$$\frac{\tau_s}{\tau_1} \ll 1, \tag{A3}$$

then $\exp(-\tau_s/\tau_1) \approx 1 - \tau_s/\tau_1$ and Eq. (A2) can be approximated as

$$\beta \approx \frac{1-\left(1-\dfrac{\tau_s}{\tau_2}\right)}{1-\left(1-\dfrac{\tau_s}{\tau_1}\right)} = \frac{\tau_1}{\tau_2} = \alpha. \tag{A4}$$

The invariant nature of the thermocouple time constant ratio[8,9] α makes β also nearly invariant, provided the smaller time constant is much bigger than τ_s.

NOMENCLATURE

a_n, b_n = difference equation ARX parameters the nth thermocouple

$\mathbf{C}$ = noise covariance matrix of beta model $\mathbf{Y}=\mathbf{X}\boldsymbol{\theta}$, where $\mathbf{C}=\mu\mathbf{C}_0$

$\mathbf{C}_0$ = normalized noise covariance matrix of beta model $\mathbf{Y}=\mathbf{X}\boldsymbol{\theta}$

$\mathbf{C}_W$ = transformed noise of covariance matrix of beta model $\mathbf{Y}=\mathbf{X}\boldsymbol{\theta}$

d = thermocouple wire diameter (m)

$\mathbf{G},\mathbf{U}_G,\mathbf{V}_G$ = GSVD matrices

$\mathbf{g}_k$ = kth generalized singular vector of $\mathbf{G}$

g = generalized singular value of $\mathbf{G}$

h = heat transfer coefficient (W/m^2 K)

J = cost function

k = sample number

K = percentage noise to signal level

ℓ = thermocouple wire length (m)

m = thermodynamic constant

N = total number of data sets

P,Q = generic signal source, generic noise source

$\mathbf{S}$ = augmented SVD matrix

$\mathbf{S}_G$ = augmented GSVD matrix

t = time (s)

T_g = gas temperature (°C)

$\hat{T}_{gn}$ = reconstructed temperature from the nth thermocouple (°C)

$\hat{T}_{g3}$ = reconstructed temperature from thermocouples 1 and 2 (°C)

T_{mn} = measured temperature from the nth thermocouple (°C)

$\mathbf{T}_{mn}(k-i)$ = N-sample vector of the nth thermocouple output (°C)

v = gas velocity (m/s)

$\mathbf{W}$ = GSVD weighting matrix

$\mathbf{X},\mathbf{Y}$ = collection of data matrices which form beta model $\mathbf{Y}=\mathbf{X}\boldsymbol{\theta}$

z^{-1} = one sample delay

Greek symbols and others

α = time constant ratio

β = ratio of b_2 to b_1

$e_{\tau n}$ = percentage time constant estimation error of the nth thermocouple (%)

$e_{\hat{\mathbf{T}}_g}$ = percentage reconstruction error level (%)

κ = thermodynamic constant

ϕ = ratio of noise variances of thermocouples 1 to 2

γ = gamma model parameter

θ = beta model parameters

τ_n = time constant of the nth thermocouple (s)

τ_s = sample interval (s)

μ = arbitrary scalar

v = factor of proportionality of $\mathbf{C}$

ω_B = bandwidth of thermocouple (Hz)

$\boldsymbol{\Sigma}_G,\boldsymbol{\Sigma}_S,\boldsymbol{\Sigma}_W$ = GSVD matrices

$\dot{f}$ = time derivative of function $f=df/dt$

$\mathbf{I}$ = $k\times k$ identity matrix

i = number of sample delay

n = nth thermocouple

$\hat{p}$ = estimated value of parameter p

Abbreviations

ARX = auto regressive model with exogenous input(s)

ARMAX = auto regressive model with moving average exogenous input(s)

DE = difference equation

GSVD = generalized singular value decomposition

GTLS = generalized total least squares

LS = least squares

OE = output error model

rms = root mean square

Ref = reference

SVD = singular value decomposition

TLS = total least squares

ZOH = zero-order hold

[1] J. C. LaRue, T. K. Deaton, and C. H. Gibson, Rev. Sci. Instrum. **46**, 757 (1975).

[2] M. Tagawa, T. Shimoji, and Y. Ohta, Rev. Sci. Instrum. **69**, 3370 (1998).

[3] M. Tagawa and Y. Ohta, Combust. Flame **109**, 549 (1997).

[4] R. J. Kee, P. G. O'Reilly, R. Fleck, and P. T. McEntee, Soc. Automotive Eng. Trans. J. Engines **107-3**, 2413 (1999).

[5] L. J. Forney and G. C. Fralick, Rev. Sci. Instrum. **65**, 3252 (1994).

[6] M. V. Heitor, A. M. K. P. Taylor, and J. H. Whitelaw, Exp. Fluids **3**, 323 (1985).

[7] D. Bradley and K. J. Matthews, J. Mech. Eng. Sci. **10**, 299 (1968).

[8] A. Dupont, P. Paranthoen, J. C. Lecordier, and P. Gajan, J. Phys. E **17**, 808 (1984).

[9] C. Petit, P. Gajan, J. C. Lecordier, and P. Paranthoen, J. Phys. E **15**, 760 (1982).

[10] T. Tsuji, Y. Nagano, and M. Tagawa, Exp. Fluids **13**, 171 (1992).

[11] H. Pfriem, Geb. Ingen. **7-2**, 85 (1936).

[12] M. Tagawa, K. Kato, and Y. Ohta, Rev. Sci. Instrum. **74**, 3171 (2003).

[13] W. C. Strahle and M. Muthukrishman, AIAA J. **14-11**, 1642 (1976).

[14] M. D. Scardron and I. Warshawsky, NACA Tech. Note **2599**, 81 (1952).

[15] P. C. F. Hung, S. McLoone, G. Irwin, and R. Kee, Proceedings of the Irish Signals and Systems Conference, Cork, Ireland, June 2002, p. 193.

[16] L. Ljung, *System Identification: Theory for the User*, 2nd ed. (Prentice-Hall, Englewood Cliffs, NJ, 1999), p. 88.

[17] P. C. F. Hung, S. McLoone, G. Irwin, and R. Kee, Proc. 13th IFAC Symposium on System Identification, Rotterdam, Netherlands, September 2003, p. 337.

[18] Y. N. Rao and J. C. Principe, Proc. IEEE Workshop on Neural Networks for Signal Processing XII, Martigny, Switzerland, September 2002, p. 259.

[19] S. V. Huffel and J. Vandewalle, *The Total Least Squares Problem: Computational Aspects and Analysis*, 1st ed. (SIAM, Philadelphia, 1991), p. 248.

[20] S. McLoone, P. C. Hung, G. Irwin, and R. Kee (submitted).